

Disorder-robust high-field superconducting phase of FeSe single crystals

Nan Zhou^{1,5}, Yue Sun^{3,*}, C. Y. Xi², Z. S. Wang², Y. F. Zhang¹, C. Q. Xu¹, Y. Q. Pan¹, J. J. Feng¹, Y. Meng¹, X. L. Yi¹, L. Pi², T. Tamegai⁴, Xiangzhuo Xing^{1,†} and Zhixiang Shi^{1‡}

¹*School of Physics and Key Laboratory of MEMS of the Ministry of Education, Southeast University, Nanjing 211189, China*

²*Anhui Province Key Laboratory of Condensed Matter Physics at Extreme Conditions, High Magnetic Field Laboratory, Chinese Academy of Sciences, Hefei 230031, China*

³*Department of Physics and Mathematics, Aoyama Gakuin University, Kanagawa 252-5258, Japan*

⁴*Department of Applied Physics, The University of Tokyo, Tokyo 113-8656, Japan and*

⁵*Institute for Solid State Physics (ISSP), The University of Tokyo, Kashiwa, Chiba 277-8581, Japan*

(Dated: July 30, 2022)

When exposed to high magnetic fields, certain materials manifest an exotic superconducting (SC) phase that attracts considerable attention. A proposed explanation of the origin of the high-field phase is the Fulde-Ferrel-Larkin-Ovchinnikov (FFLO) state. This state is characterized by inhomogeneous superconductivity, where the Cooper pairs have finite center-of-mass momenta. Recently, the high-field phase has been observed in FeSe, and it was deemed to originate from the FFLO state. Here, we synthesized FeSe single crystals with different levels of disorders. The level of disorder is expressed by the ratio of the mean free path to the coherence length and ranges between 35 and 1.2. The upper critical field B_{c2} was systematically studied over a wide range of temperatures, which went as low as ~ 0.5 K, and magnetic fields, which went up to ~ 38 T along the c axis and in the ab plane. In the high-field region parallel to the ab plane, an unusual SC phase was confirmed in all the crystals, and the phase was found to be robust to disorders. This result suggests that the high-field SC state in FeSe may not be a FFLO state, which should be sensitive to disorders.

The orbital and Pauli-paramagnetic pair-breaking effects are two distinct mechanisms for destroying superconductivity and limiting the maximum upper critical field in type-II superconductors [1, 2]. However, triggered by certain conditions, some unconventional superconductors can easily overcome the Pauli limitation by forming an exotic SC phase [3–24]. Among them, an inhomogeneous SC state occurs when Pauli pair-breaking effect dominates over orbital pair-breaking effect, which is independently predicted by Fulde and Ferrell [3], and Larkin and Ovchinnikov [4] (FFLO state) half a century ago. In the FFLO state, the Zeeman-split Fermi surfaces could drive the formation of Cooper pairs with a finite center-of-mass momenta, thus realizing a spatially modulated SC state. The large Maki parameter α , clean limit (mean free path $\ell \gg$ coherence length ξ), and unconventional pairing symmetries [6] could drive a system easier access to the FFLO state. In previous reports, the FFLO state was suggested to exist in heavy-fermion [5–7], organic [8–18], and some iron-based superconductors [19–22]. In the heavy fermion superconductor CeCoIn₅, an additional spin-density wave (SDW) has been observed to coexist with SC [23, 24], implying that the high-field phase does not simply originate from the FFLO state. In contrast, in some layered organic superconductors, the FFLO state was observed without any magnetic order [8–18].

The target material of this study is the iron chalcogenide superconductor FeSe [25], which has attracted considerable interest due to its unique electrical properties, such as multiband structure [26], electronic nematicity [27], extremely small Fermi energy [21], and strongly orbital-dependent pairing mechanism [28]. Recently, a

high-field SC phase has been observed in FeSe at temperatures below 2 K and under the applied field close to the upper critical field [19, 20]. It has been suggested that the high-field SC phase may originate from the FFLO state [19, 20].

Since the phase transition from FFLO to the Bardeen-Cooper-Schrieffer (BCS) state is of the first order, the FFLO state is readily destroyed by disorders [6, 29, 30]. Therefore, the disorder effect can be a useful method to clarify whether the high-field SC phase in FeSe stems from the FFLO state. In this study, we probed the high-field SC phase in three FeSe single crystals with a disorder level ℓ/ξ ranging from 35 to 1.2. We found that the high-field SC phase exists in all the three crystals and is robust against disorders.

The single crystals of FeSe studied here were synthesized by the vapor transport method [31, 32]. Single crystals with different amounts of disorders were selected from different batches. The structure of FeSe single crystals was characterized by X-ray diffraction (XRD) with Cu- $K\alpha$ radiation. The crystal composition was determined by energy-dispersive X-ray spectroscopy (EDX). Temperature dependence of the resistivity up to 9 T was measured by using a physical property measurement system (PPMS, Quantum Design). The magnetization was measured by a commercial SC quantum interference device magnetometer (MPMS-XL5, Quantum Design). The high-field transport measurements were carried out using standard a.c. lock-in techniques with a ³He cryostat and a dc-resistive magnet (up to 38 T) at the High Magnetic Field Laboratory of Chinese Academy of Sciences.

Figure 1(a) shows the zero-field resistivity $\rho(T)$ for the

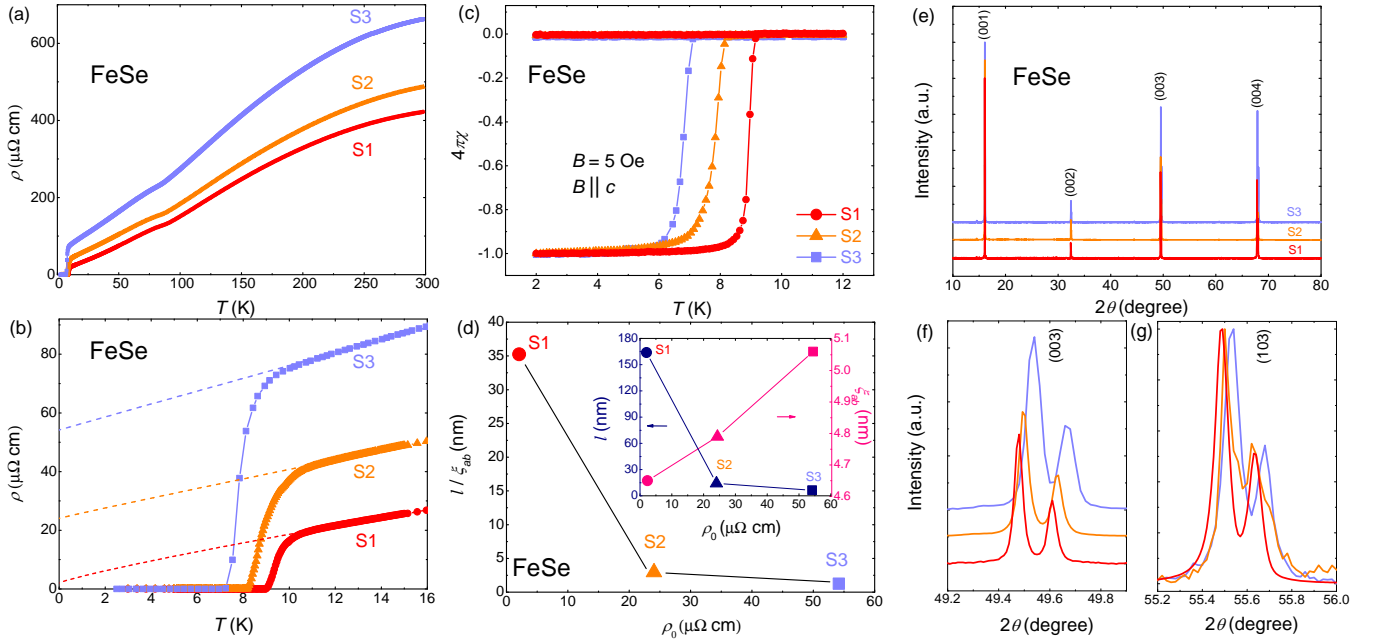


FIG. 1. Temperature dependencies of the resistivity at zero field in the temperature ranges of (a) 0-300 K, (b) below 16 K for three selected FeSe single crystals with different amounts of disorders. The dashed lines correspond to the power-law fitting $\rho(T) = \rho_0 + AT^\alpha$. (c) Temperature dependence of magnetic susceptibility χ measured under 5 Oe field along c axis. (d) Residual resistivity ρ_0 dependence of the ratio of the mean free path ℓ to the coherence length ξ_{ab} . The inset displays the ρ_0 dependence of ℓ (left axis) and the ξ_{ab} (right axis). (e) The single-crystal XRD patterns for the three selected FeSe single crystals. The enlarged diffraction peaks of (f) (003) and (g) (103).

three selected FeSe single crystals. As shown in Fig. 1(b), the SC transition temperature T_c determined by the zero resistivity is ~ 9.0 K (sample S1), 8.2 K (sample S2) and 7.1 K (sample S3). The residual resistivity ρ_0 is determined by using the power-law fitting $\rho(T) = \rho_0 + AT^\alpha$ (ρ_0 , A , and α as the fitting parameters) from normal state data to zero temperature as shown by the dashed lines in Fig. 1(b). The obtained ρ_0 is $\sim 2.1 \mu\Omega \text{ cm}$ (sample S1), $24 \mu\Omega \text{ cm}$ (sample S2) and $54.2 \mu\Omega \text{ cm}$ (sample S3), respectively. The residual resistivity ratio (RRR), defined as ρ_{300K}/ρ_0 , is estimated as ~ 207 for sample S1, ~ 20.3 for sample S2, and ~ 12.2 for sample S3 (Table I). A kink-like behavior at $T \sim 90$ K related to the structural transition [33] could be seen more clearly in the plot of $d\rho/dT$ as shown in Fig. S1 [34]. The structural transition temperature T_s is found to be slightly suppressed by the disorders, which is consistent with previous reports [32].

Superconductivity was confirmed by the temperature dependence of the susceptibility measurements as shown in Fig. 1(c). The obtained T_c that is defined as the deviation of the zero-field-cooling and field-cooling susceptibilities is in good agreement with the resistivity data. The sharp SC transition width indicates the homogeneous distribution of disorders.

We estimated the mean free path by assuming that the hole and electron pockets are compensated perfectly. According to the expressions $\ell = \frac{\pi c \hbar}{N e^2 k_F \rho_0}$ [20], where c is the lattice parameter, N is the number of formula units per unit cell, $k_F = 1.07 \text{ nm}^{-1}$ [20] is the Fermi wave vector, and ρ_0 is the residual resistivity, ℓ is estimated as ~ 164 , 14.1 and 6.3 nm for sample S1, S2, and S3, respectively (see the inset of Fig. 1(d)). The ratio of the mean free path ℓ to the in-plane coherence length ξ_{ab} is presented in the main panel of Fig. 1(d) and Table I. The estimation of ξ_{ab} will be discussed later. Our results confirm that sample S1 is in the clean limit with $\ell/\xi_{ab} > 35$. By contrast, considerable amounts of disorders have been successfully introduced into sample S2 and S3 because ℓ/ξ_{ab} is reduced to ~ 3.0 and 1.2, respectively.

We conducted structure and composition analyses to obtain further information about the disorders in the three crystals [see Fig. 1(e)]. Only the $(00l)$ peaks are observed for all the three crystals, which can be well indexed based on a tetragonal structure with the $(P4/nmm)$ space group. The positions of peaks were found to be slightly shifted to a higher angle from S1 to S3, which can be seen more clearly in the enlarged part of (003) peaks shown in Fig. 1(f). To obtain the lattice constant a/b , we measured (103) peaks by scanning the

TABLE I. Summary of the experimentally derived parameters for samples S1, S2, and S3. T_c , the temperature for the resistivity deviates from the SC state; ρ_0 , residual resistivity; RRR , residual resistivity ratio; α , Maki parameter; $B_{c2}^c(0)$ and $B_{c2}^{ab}(0)$ are the estimated upper critical fields along c axis, and in the ab plane. ℓ , the mean free path; $\xi_c(0)$ and $\xi_{ab}(0)$ the coherence length along c axis and in the ab plane are determined from $B_{c2}^c(0)$ and $B_{c2}^{ab}(0)$. $\ell/\xi_{ab}(0)$, the ratio of the mean free path ℓ to the coherence length $\xi_{ab}(0)$.

	T_c (K)	ρ_0 ($\mu\Omega$ cm)	RRR	α	$B_{c2}^c(0)$ (T)	$B_{c2}^{ab}(0)$ (T)	ℓ (nm)	$\xi_c(0)$ (nm)	$\xi_{ab}(0)$ (nm)	$\ell/\xi_{ab}(0)$
S1	9.0	2.1	207	1.13	15.26	27.21	164	2.6	4.7	35.2
S2	8.2	24	20.3	1.32	14.33	25.28	14.1	2.7	4.8	3.0
S3	7.1	54.2	12.2	1.48	12.86	22.27	6.3	2.9	5.1	1.2

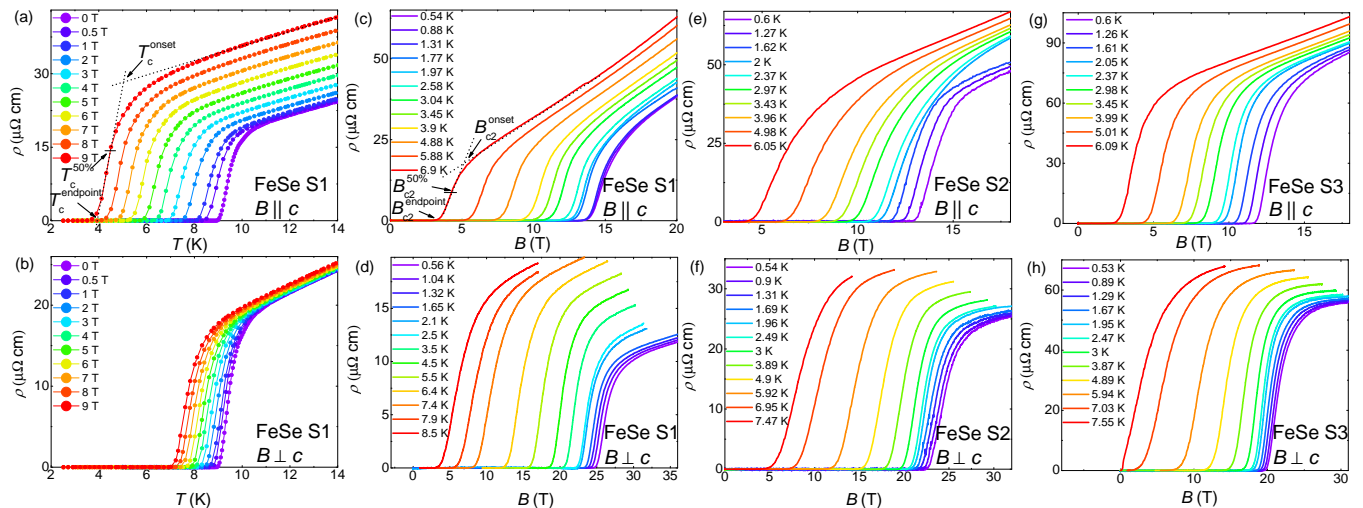


FIG. 2. Temperature dependence of the resistivity for sample 1 with (a) $B \parallel c$ (b) $B \perp c$ under fields from 0 to 9 T. Magnetic field dependence of the resistivity with $B \parallel c$ and $B \perp c$ at several temperatures for (c-d) sample 1, (e-f) sample 2, and (g-h) sample 3.

crystal angle ω independently of 2θ (angle between incident and scattered X-rays), as shown in Fig. 1(g). The lattice constants are estimated as $a = (3.777 \pm 0.002) \text{ \AA}$, $c = (5.524 \pm 0.002) \text{ \AA}$ for sample S1, $a = (3.765 \pm 0.002) \text{ \AA}$, $c = (5.521 \pm 0.002) \text{ \AA}$ for sample S2, and $a = (3.761 \pm 0.002) \text{ \AA}$, $c = (5.519 \pm 0.002) \text{ \AA}$ for sample S3, respectively. Both a and c decrease with increasing disorders, indicating lattice shrinkage. The EDX measurements show that the molar ratio of Fe : Se is $\sim 1 : 1.005$, $1 : 1.074$, and $1 : 1.087$ for samples S1, S2, and S3, respectively, which indicates that the amount of Fe is less than the amount of Se, and the amount of Fe decreases with increasing disorders. The lattice shrinkage and the smaller amount of Fe suggest that the disorders could be Fe vacancies, which has been confirmed by the scanning tunneling microscopy (STM) measurements [35].

Both the temperature (up to 9 T) and magnetic field (up to 38 T) dependencies of resistivity were measured to probe the upper critical fields of the three crystals. The determinations of B_{c2} by the criteria of onset, 50%, and the end point of the SC transition are shown in Figs. 2(a)

and 2(c). In the following main text, B_{c2} determined by the criterion of 50% of the SC transition is adopted for discussion. While, the B_{c2} obtained by the criteria of the onset and end point of the SC transition were presented in Fig. S3 [34]. Here, we want to emphasize that our conclusion is not affected by the criteria of B_{c2} .

B_{c2} of the three crystals are shown in Figs. 3(a)–(c). The anisotropy $\gamma = B_{c2}^{ab}/B_{c2}^c$ is found to be slightly increased in crystals with more disorders (see Fig. S5(d) [34]). The zero-temperature coherence length was estimated by using $\xi_{ab}(0) = (\Phi_0/2\pi B_{c2}^c(0))^{1/2}$ and $\xi_c(0) = \Phi_0/2\pi \xi_{ab}(0) B_{c2}^{ab}(0)$ ($\Phi_0 = 2.07 \times 10^{-15} \text{ Wb}$ is the magnetic flux quantum). Herein, we extract the $B_{c2}^c(0)$ from the two-band fitting for estimating the coherence lengths, with $\xi_{ab}(0) \sim 4.7 \text{ nm}$ (S1), 4.8 nm (S2), and 5.1 nm (S3), respectively. The $B_{c2}^{ab}(0)$ is estimated by linearly extrapolating the low temperature upper critical field data to zero temperature, obtains the $\xi_c(0) \sim 2.6 \text{ nm}$ (S1), 2.7 nm (S2), and 2.9 nm (S3), respectively (see Table I and Fig. S4 [34]). Meanwhile, the coherence lengths are also estimated by using the anisotropic Ginzburg-Landau

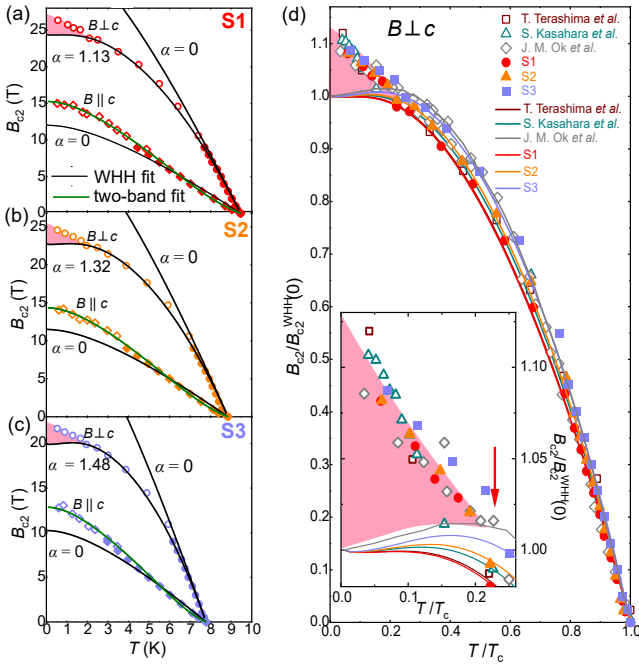


FIG. 3. [(a)–(c)] Temperature dependencies of the upper critical field $B_{c2}(T)$ for the three selected FeSe single crystals. Symbols of the diamond and circle represent the case of $B \parallel c$ and $B \perp c$, respectively. The two-band model (green lines) and WHH fitting curves (black lines) are shown for $B \parallel c$ and $B \perp c$. Meanwhile, the WHH model predictions with $\alpha = 0$ are also presented for comparison. (d) The critical field B_{c2} normalized by the $B_{c2}^{\text{WHH}}(0 \text{ K})$ for the crystals used in this paper and the previous works [19, 20, 36]. The solid lines represent the WHH fitting. The inset shows the enlarged low temperature part.

equations (see Fig. S5 [34]).

For $B \parallel c$, the experimental data B_{c2}^c for the three crystals is well above the predicted upper limit based on the Werthamer-Helfand-Hohenberg (WHH) theory [1] with Maki parameter $\alpha = 0$, and spin orbit interaction $\lambda = 0$ (shown as the black lines), and manifests a convex increase at $T > 4 \text{ K}$ but a concave increase at $T < 4 \text{ K}$. Similar behavior has also been observed in other IBSSs [37, 38], which can be well reproduced by the two-band model (shown as the green lines). For $B \parallel ab$, the experimental data B_{c2}^{ab} falls below the WHH prediction at low temperatures with $\alpha = 0$ and $\lambda_{\text{so}} = 0$, indicating that the spin-paramagnetic effect cannot be ignored. By considering a finite α (λ keeps as 0), the WHH model can fit the B_{c2}^{ab} well in the temperature range of $T > 2 \text{ K}$. The Maki parameter α extracted from the WHH fitting is plotted in Fig. S5(e) [34], which is increased with ρ_0 (Table I).

Interestingly, at $T < 2 \text{ K}$, the experimental data significantly deviates from the WHH curves, and displays

an unusual upturn for all the three crystals. This phenomenon was also observed in previous studies, and was predicted to be originated from a new high-field SC phase [19, 20]. To directly compare the high-field SC phase for crystals with different amounts of disorders, B_{c2}^{ab} normalized by the $B_{c2,ab}^{\text{WHH}}(0 \text{ K})$ (WHH fitting with finite α) are shown in Fig. 3(d). The upper critical field B_{c2}^{ab} reported by T. Terashima *et al.* (open squares) [36], S. Kasahara *et al.* (open triangles) [20] and J. M. Ok *et al.* (open diamonds) [19] are also incorporated for comparison. Crystals used in those reports are supposed to contain different amounts of disorders. Obviously, the upturn behavior was observed in the B_{c2}^{ab} for all the crystals. Furthermore, the enhancements of B_{c2}^{ab} above the WHH fitting for different crystals are almost identical, which can be seen clearly in the inset of Fig. 3(d).

Since the FFLO state is very sensitive to disorders [6, 29, 30], it can only exist in crystals in the clean limit, which is in stark contrast to our observation of the disorder-robust high-field phase. Therefore, the observed high-field SC phase seems not to be a FFLO state, although in some theoretically predicted special cases, the FFLO state can survive under moderate disorder strength [39] or is a second-order phase transition being more robust against disorders [40].

Another possible origin of the high-field SC phase is the coexistence of the SDW order, which is triggered by the nesting effect around the nodal position of SC gap [41]. The SDW order has been discussed as another possible mechanism for the high-field phase in heavy fermion superconductor CeCoIn_5 beside the FFLO state [23, 41]. Theoretical calculation proposed that the SDW order close to B_{c2} is a direct result of the strong spin-paramagnetic pair-breaking effect and nodal gap structure [42]. In FeSe, the gap nodes or deep minima in both the electron-type ϵ -band with small gap size and the hole-type α -band with large gap size have already been confirmed [21, 28, 43], which makes the field-induced SDW order possible. Such a kind of SDW order coexisting with superconductivity should be sensitive to the gap structure. If the nodes or gap minima are smeared out, such a SDW order will disappear spontaneously. Our previous work has observed that the nodes or gap minima in the small ϵ -gap can be smeared out by disorders [44]. However, the nodes or gap minima in the large α -gap should be more robust against disorders because the v-shape spectrum was observed on the STM measurements in the FeSe crystals with high level of S-doping [45]. Since the high-field SC phase in FeSe is only observed at fields close to B_{c2} , it should be attributed to the larger α -gap. Therefore, our observation of the disorder-robust behavior is not contradictory to the SDW order induced in the high-field phase. Further efforts such as nuclear magnetic resonance and neutron diffraction measurements are required to clarify the origin of the high-field SC phase in FeSe. Nevertheless, our observations suggest that FeSe

provides an intriguing platform to study the interplay between multiple phases such as superconductivity, nematicity, and the SDW or FFLO state.

To conclude, we studied the upper critical fields of FeSe single crystals with different amounts of disorders. A high-field SC phase was observed in all the crystals, and it was found to be robust against disorders. These results suggest that the high-field SC state in FeSe may not be from the FFLO state. Therefore, the high-field phase should be related to a disorder-robust order, which may provide new clues to understand the exotic properties of FeSe.

The authors would like to thank Shigeru Kasahara for stimulating discussions. A portion of this work was performed on the Steady High Magnetic Field Facilities, High Magnetic Field Laboratory, Chinese Academy of Sciences, and supported by the High Magnetic Field Laboratory of Anhui Province. This work was partly supported by the National Key R&D Program of China (Grant No. 2018YFA0704300), the Strategic Priority Research Program (B) of the Chinese Academy of Sciences (Grant No. XDB25000000), the National Natural Science Foundation of China (Grant No. U1932217, No. 11674054, and No. 11874359), and JSPS KAKENHI (No. JP20H05164, No. JP19K14661, and No. JP17H01141).

N. Z. and Y. S. contributed equally to this paper.

* Corresponding author: sunyue@phys.aoyama.ac.jp

† Corresponding author: xzxing@seu.edu.cn

‡ Corresponding author: zxshi@seu.edu.cn

- [1] N. Werthamer, E. Helfand, and P. Hohenberg, *Phys. Rev.* **147**, 295 (1966).
- [2] N. Zhou, X. Xu, J. Wang, J. Yang, Y. Li, Y. Guo, W. Yang, C. Niu, B. Chen, C. Cao, *et al.*, *Phys. Rev. B* **90**, 094520 (2014).
- [3] P. Fulde and R. A. Ferrell, *Phys. Rev.* **135**, A550 (1964).
- [4] A. Larkin and Y. N. Ovchinnikov, *Sov. Phys. JETP* **20**, 762 (1965).
- [5] S. Kitagawa, G. Nakamine, K. Ishida, H. Jeevan, C. Geibel, and F. Steglich, *Phys. Rev. Lett.* **121**, 157004 (2018).
- [6] Y. Matsuda and H. Shimahara, *J. Phys. Soc. Jpn.* **76**, 051005 (2007).
- [7] A. Bianchi, R. Movshovich, C. Capan, P. Pagliuso, and J. Sarrao, *Phys. Rev. Lett.* **91**, 187004 (2003).
- [8] J. Singleton, J. Symington, M. Nam, A. Ardavan, M. Kurmoo, and P. Day, *J. Phys.: Condens. Matter* **12**, L641 (2000).
- [9] R. Lortz, Y. Wang, A. Demuer, P. Böttger, B. Bergk, G. Zwicky, Y. Nakazawa, and J. Wosnitza, *Phys. Rev. Lett.* **99**, 187002 (2007).
- [10] B. Bergk, A. Demuer, I. Sheikin, Y. Wang, J. Wosnitza, Y. Nakazawa, and R. Lortz, *Phys. Rev. B* **83**, 064506 (2011).
- [11] R. Beyer, B. Bergk, S. Yasin, J. Schlueter, and J. Wosnitza, *Phys. Rev. Lett.* **109**, 027003 (2012).
- [12] G. Koutroulakis, H. Kühne, J. Schlueter, J. Wosnitza, and S. Brown, *Phys. Rev. Lett.* **116**, 067003 (2016).
- [13] S. Tsuchiya, J.-i. Yamada, K. Sugii, D. Graf, J. S. Brooks, T. Terashima, and S. Uji, *J. Phys. Soc. Jpn.* **84**, 034703 (2015).
- [14] C. Agosta, J. Jin, W. Coniglio, B. Smith, K. Cho, I. Stroe, C. Martin, S. Tozer, T. Murphy, E. Palm, *et al.*, *Phys. Rev. B* **85**, 214514 (2012).
- [15] J. Wright, E. Green, P. Kuhns, A. Reyes, J. Brooks, J. Schlueter, R. Kato, H. Yamamoto, M. Kobayashi, and S. Brown, *Phys. Rev. Lett.* **107**, 087002 (2011).
- [16] H. Mayaffre, S. Krämer, M. Horvatić, C. Berthier, K. Miyagawa, K. Kanoda, and V. Mitrović, *Nat. Phys.* **10**, 928 (2014).
- [17] K. Cho, B. Smith, W. Coniglio, L. Winter, C. Agosta, and J. Schlueter, *Phys. Rev. B* **79**, 220507 (2009).
- [18] W. A. Coniglio, L. E. Winter, K. Cho, C. Agosta, B. Fravel, and L. Montgomery, *Phys. Rev. B* **83**, 224507 (2011).
- [19] J. M. Ok, C. I. Kwon, Y. Kohama, J. S. You, S. K. Park, J.-h. Kim, Y. Jo, E. Choi, K. Kindo, W. Kang, *et al.*, *Phys. Rev. B* **101**, 224509 (2020).
- [20] S. Kasahara, Y. Sato, S. Licciardello, M. Čulo, S. Arsenijević, T. Ottenbros, T. Tominaga, J. Böker, I. Eremin, T. Shibauchi, *et al.*, *Phys. Rev. Lett.* **124**, 107001 (2020).
- [21] S. Kasahara, T. Watashige, T. Hanaguri, Y. Kohsaka, T. Yamashita, Y. Shimoyama, Y. Mizukami, R. Endo, H. Ikeda, K. Aoyama, *et al.*, *Proc. Natl. Acad. Sci. U. S. A.* **111**, 16309 (2014).
- [22] C.-w. Cho, J. H. Yang, N. F. Yuan, J. Shen, T. Wolf, and R. Lortz, *Phys. Rev. Lett.* **119**, 217002 (2017).
- [23] M. Kenzelmann, T. Strässle, C. Niedermayer, M. Sgrist, B. Padmanabhan, M. Zolliker, A. Bianchi, R. Movshovich, E. D. Bauer, J. L. Sarrao, *et al.*, *Science* **321**, 1652 (2008).
- [24] M. Kenzelmann, S. Gerber, N. Egetenmeyer, J. Gavilano, T. Strässle, A. Bianchi, E. Ressouche, R. Movshovich, E. Bauer, J. Sarrao, *et al.*, *Phys. Rev. Lett.* **104**, 127001 (2010).
- [25] F.-C. Hsu, J.-Y. Luo, K.-W. Yeh, T.-K. Chen, T.-W. Huang, P. M. Wu, Y.-C. Lee, Y.-L. Huang, Y.-Y. Chu, D.-C. Yan, *et al.*, *Proc. Natl. Acad. Sci. U. S. A.* **105**, 14262 (2008).
- [26] M. Watson, T. Yamashita, S. Kasahara, W. Knafo, M. Nardone, J. Béard, F. Hardy, A. McCollam, A. Narayanan, S. Blake, *et al.*, *Phys. Rev. Lett.* **115**, 027006 (2015).
- [27] S. Hosoi, K. Matsuura, K. Ishida, H. Wang, Y. Mizukami, T. Watashige, S. Kasahara, Y. Matsuda, and T. Shibauchi, *Proc. Natl. Acad. Sci. U. S. A.* **113**, 8139 (2016).
- [28] P. O. Sprau, A. Kostin, A. Kreisel, A. E. Böhmer, V. Taufour, P. C. Canfield, S. Mukherjee, P. J. Hirschfeld, B. M. Andersen, and J. S. Davis, *Science* **357**, 75 (2017).
- [29] L. Aslamazov, *Sov. Phys. JETP* **28**, 773 (1969).
- [30] S. Takada, *Prog. Theor. Phys.* **43**, 27 (1970).
- [31] Y. Sun, S. Pyon, and T. Tamegai, *Phys. Rev. B* **93**, 104502 (2016).
- [32] A. Böhmer, V. Taufour, W. Straszheim, T. Wolf, and P. Canfield, *Phys. Rev. B* **94**, 024526 (2016).
- [33] T. McQueen, A. Williams, P. Stephens, J. Tao, Y. Zhu, V. Ksenofontov, F. Casper, C. Felser, and R. J. Cava, *Phys. Rev. Lett.* **103**, 057002 (2009).
- [34] See Supplemental Material at [] for the first derivative of $\rho-T$, temperature dependent resistivity at various fixed

- fields, the B_{c2} determined by the criterion of onset and offset, the estimation of the $B_{c2}^{\parallel ab}$ (0 K), the coherence length, anisotropy, and Maki parameter.
- [35] L. Jiao, S. Rößler, C. Koz, U. Schwarz, D. Kasinathan, U. K. Rößler, and S. Wirth, *Phys. Rev. B* **96**, 094504 (2017).
- [36] T. Terashima, N. Kikugawa, A. Kiswandhi, E.-S. Choi, J. S. Brooks, S. Kasahara, T. Watashige, H. Ikeda, T. Shibauchi, Y. Matsuda, *et al.*, *Phys. Rev. B* **90**, 144517 (2014).
- [37] T. Wang, C. Zhang, L. Xu, J. Wang, S. Jiang, Z. Zhu, Z. Wang, J. Chu, J. Feng, L. Wang, *et al.*, *Sci. China-Phys. Mech. Astron.* **63**, 227412 (2020).
- [38] X. Xing, W. Zhou, J. Wang, Z. Zhu, Y. Zhang, N. Zhou, B. Qian, X. Xu, and Z. Shi, *Sci. Rep.* **7**, 45943 (2017).
- [39] A. Vorontsov, J. Sauls, and M. Graf, *Phys. Rev. B* **72**, 184501 (2005).
- [40] Q. Cui and K. Yang, *Phys. Rev. B* **78**, 054501 (2008).
- [41] M. Kenzelmann, *Rep. Prog. Phys.* **80**, 034501 (2017).
- [42] R. Ikeda, Y. Hatakeyama, and K. Aoyama, *Phys. Rev. B* **82**, 060510 (2010).
- [43] Y. Sun, S. Kittaka, S. Nakamura, T. Sakakibara, K. Irie, T. Nomoto, K. Machida, J. Chen, and T. Tamegai, *Phys. Rev. B* **96**, 220505 (2017).
- [44] Y. Sun, S. Kittaka, S. Nakamura, T. Sakakibara, P. Zhang, S. Shin, K. Irie, T. Nomoto, K. Machida, J. Chen, and T. Tamegai, *Phys. Rev. B* **98**, 064505 (2018).
- [45] T. Hanaguri, K. Iwaya, Y. Kohsaka, T. Machida, T. Watashige, S. Kasahara, T. Shibauchi, and Y. Matsuda, *Sci. Adv.* **4**, eaar6419 (2018).